Tunable Band Alignment and Photovoltaic Potential in a Type-II $Sb_2S_3/SnSe_2$ Heterostructure

Sixuan Huang[1], Li Fang[1]*, GuoRui Rao[1], GuangZhaoWang[2], Hui Lv[1,3]

[1]*National "111 Research Center" Microelectronics and Integrated Circuits, School of Science, Hubei University of Technology, Wuhan, 430068, PR China*

[2]*Key Laboratory of Extraordinary Bond Engineering and Advanced Materials Technology of Chongqing, School of Electronic Information Engineering, Yangtze Normal University, Chongqing, 408100, PR China*

[3]*Hubei University of Education, Wuhan, 430068, PR China*

[*]*Corresponding author email: fangli@hbut.edu.cn*

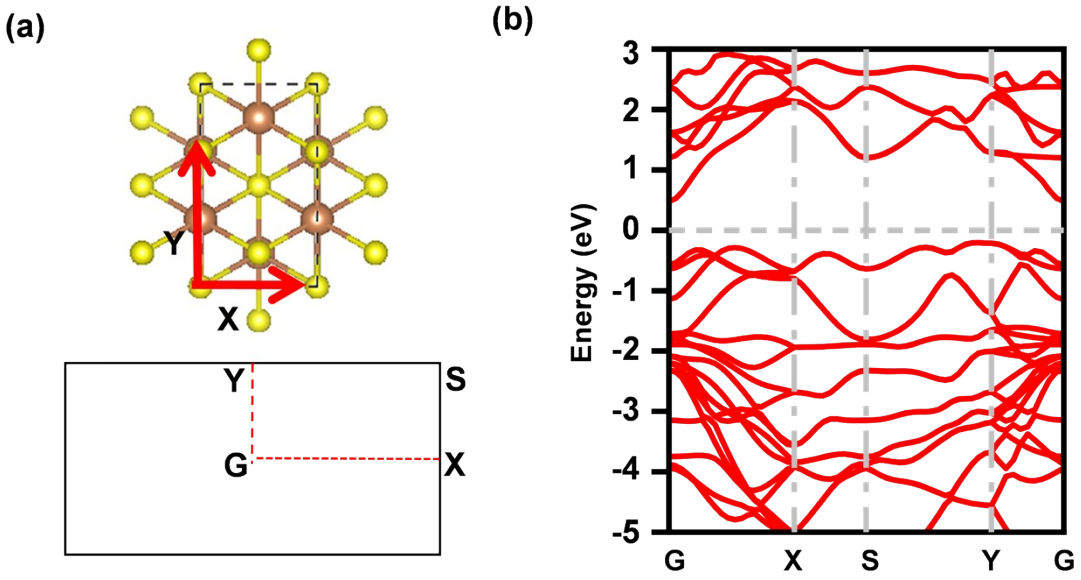

Figure S1 (a) Crystal structure of Sb_2S_3 hexagonal cell and high-symmetry points in the Brillouin zone. (b) Band structure of the Sb_2S_3 hexagonal cell.

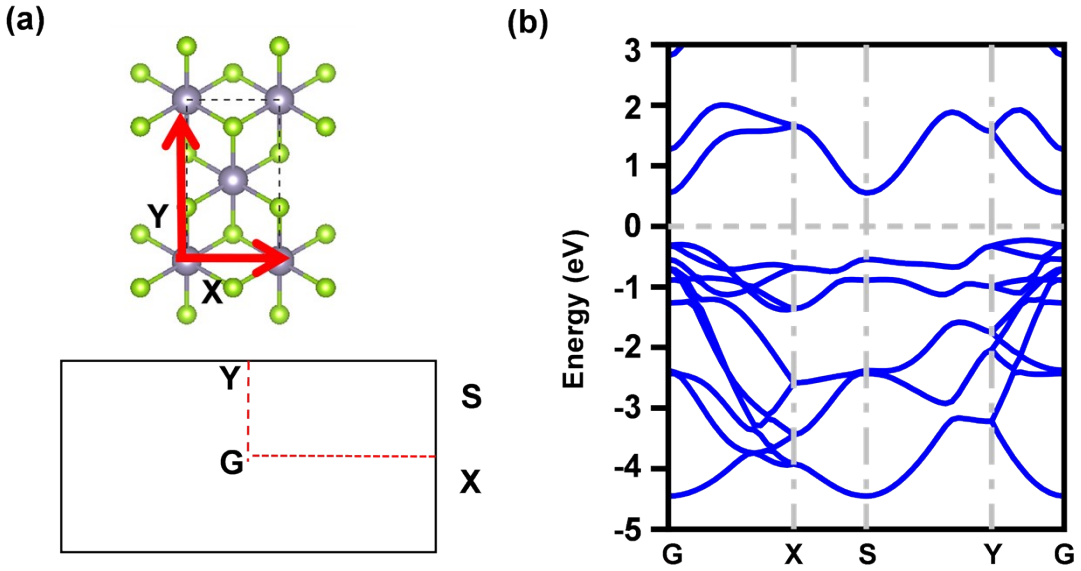

Figure S2 (a) Crystal structure of $SnSe_2$ hexagonal cell and high-symmetry points in the Brillouin zone. (b) Band structure of the $SnSe_2$ hexagonal cell.

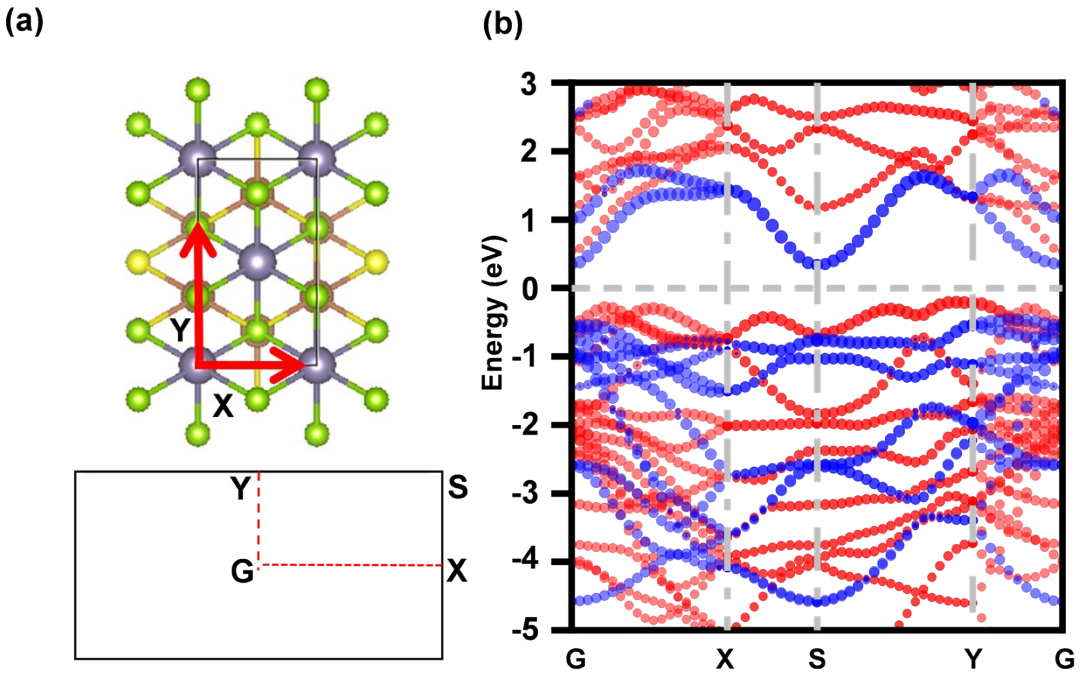

Figure S3 (a) Crystal structure of $Sb_2S_3/SnSe_2$ hexagonal cell and high-symmetry points in the Brillouin zone. (b) Band structure of the $Sb_2S_3/SnSe_2$ hexagonal cell.

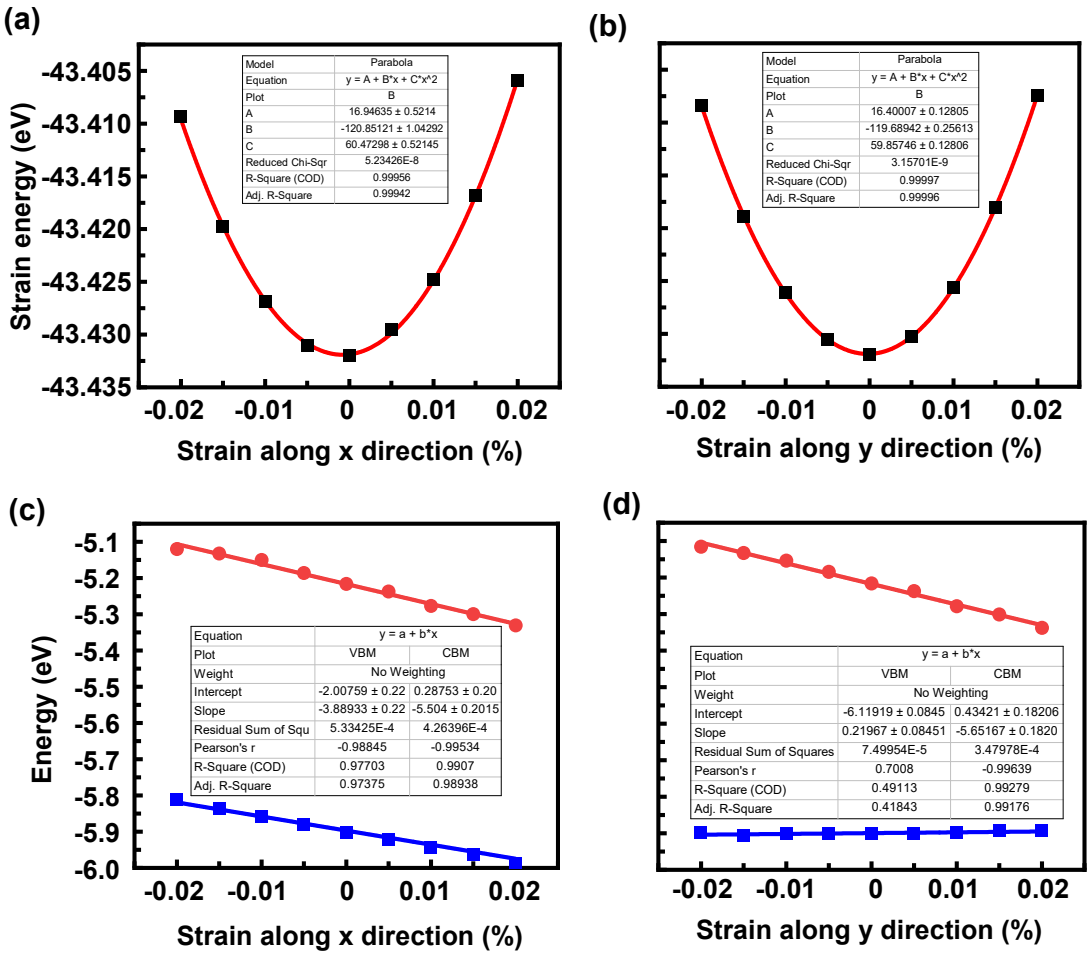

Figure S4 In-plane stiffness and deformation potential of the Sb_2S_3 monolayer obtained from the PBE functional. (a) and (b) are the elastic moduli along the x and y directions, respectively. (c) and (d) are the corresponding deformation potentials for the CBM and VBM.

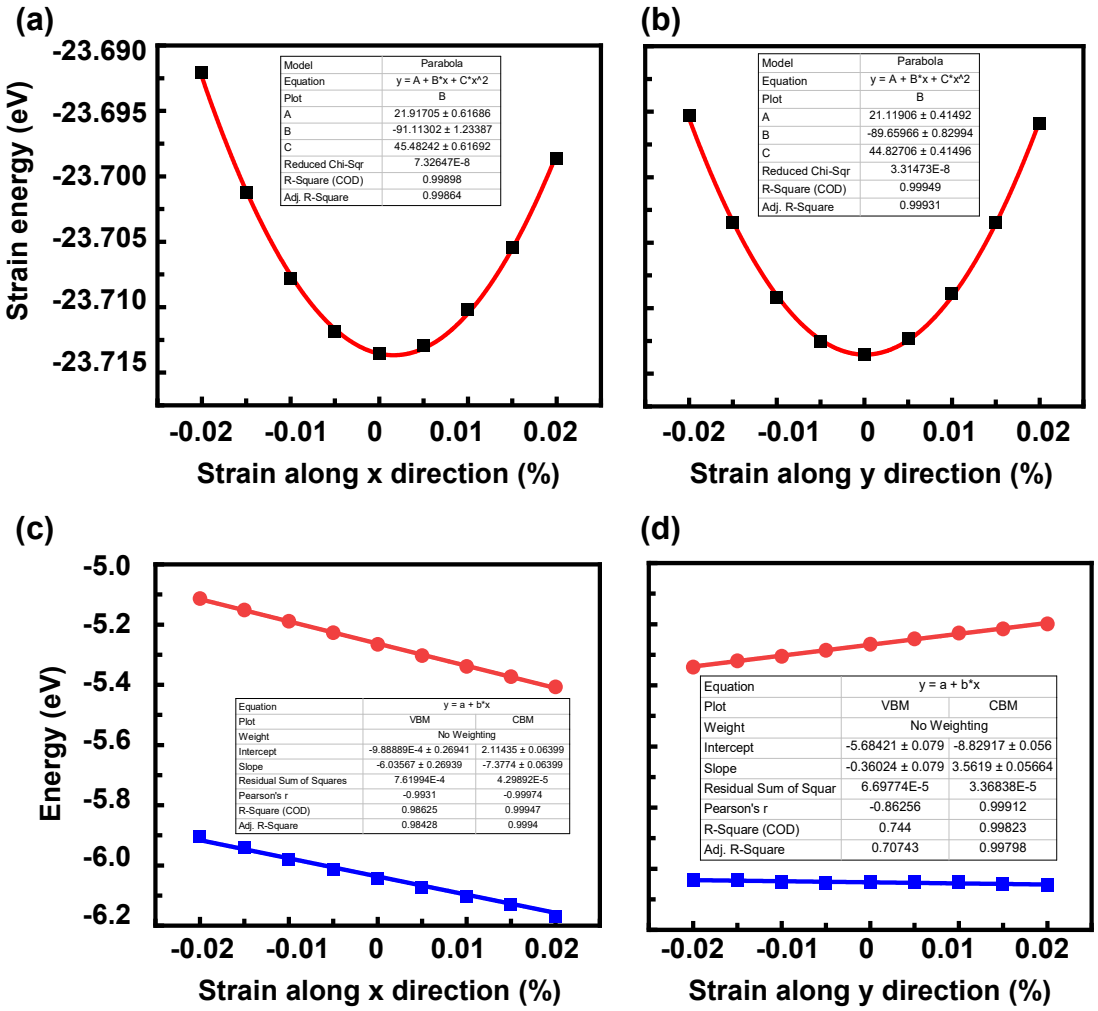

Figure S5 In-plane stiffness and deformation potential of the $SnSe_2$ monolayer obtained from the PBE functional. (a) and (b) are the elastic moduli along the x and y directions, respectively. (c) and (d) are the corresponding deformation potentials for the CBM and VBM.

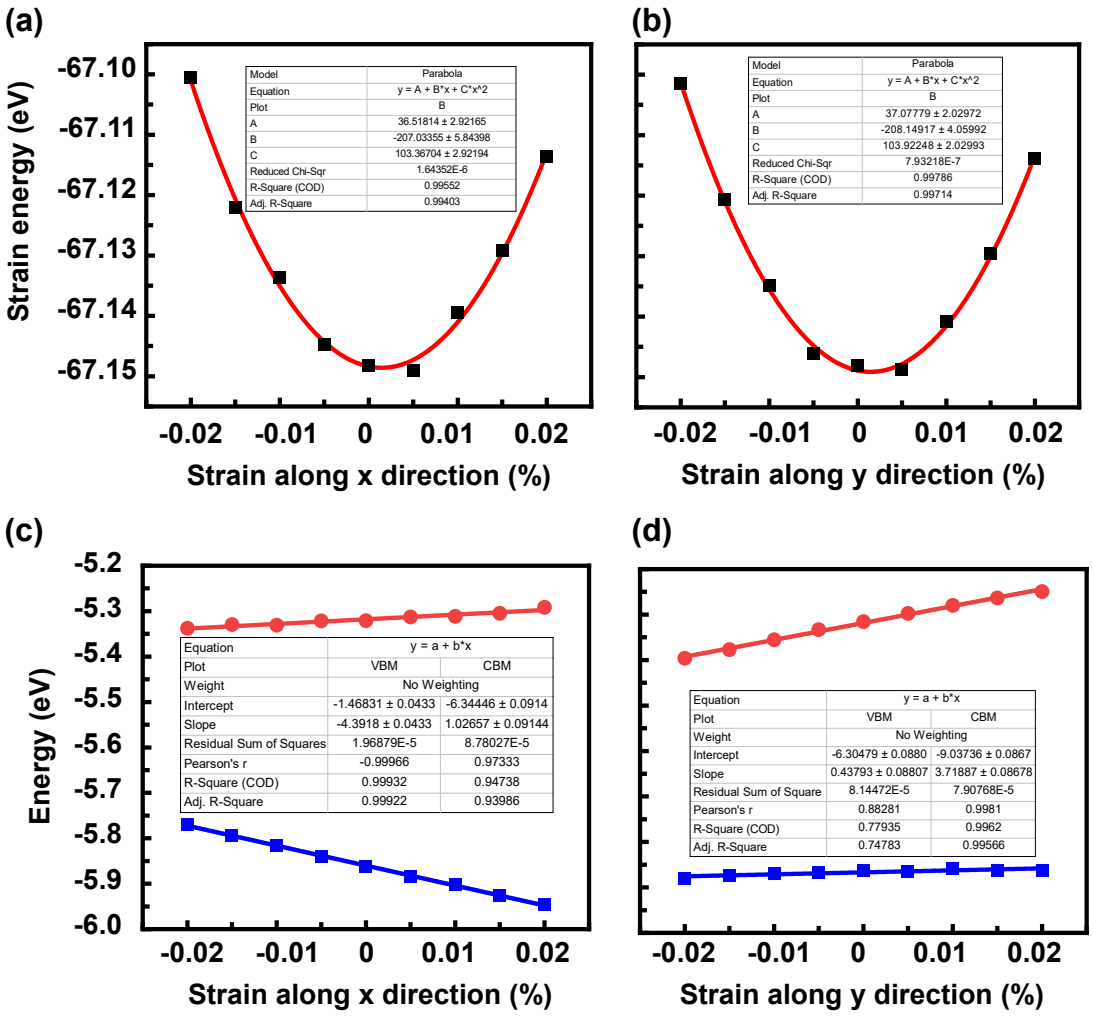

Figure S6 In-plane stiffness and deformation potential of the $Sb_2S_3/SnSe_2$ heterostructure obtained from the PBE functional. (a) and (b) are the elastic moduli along the x and y directions, respectively. (c) and (d) are the corresponding deformation potentials for the CBM and VBM.

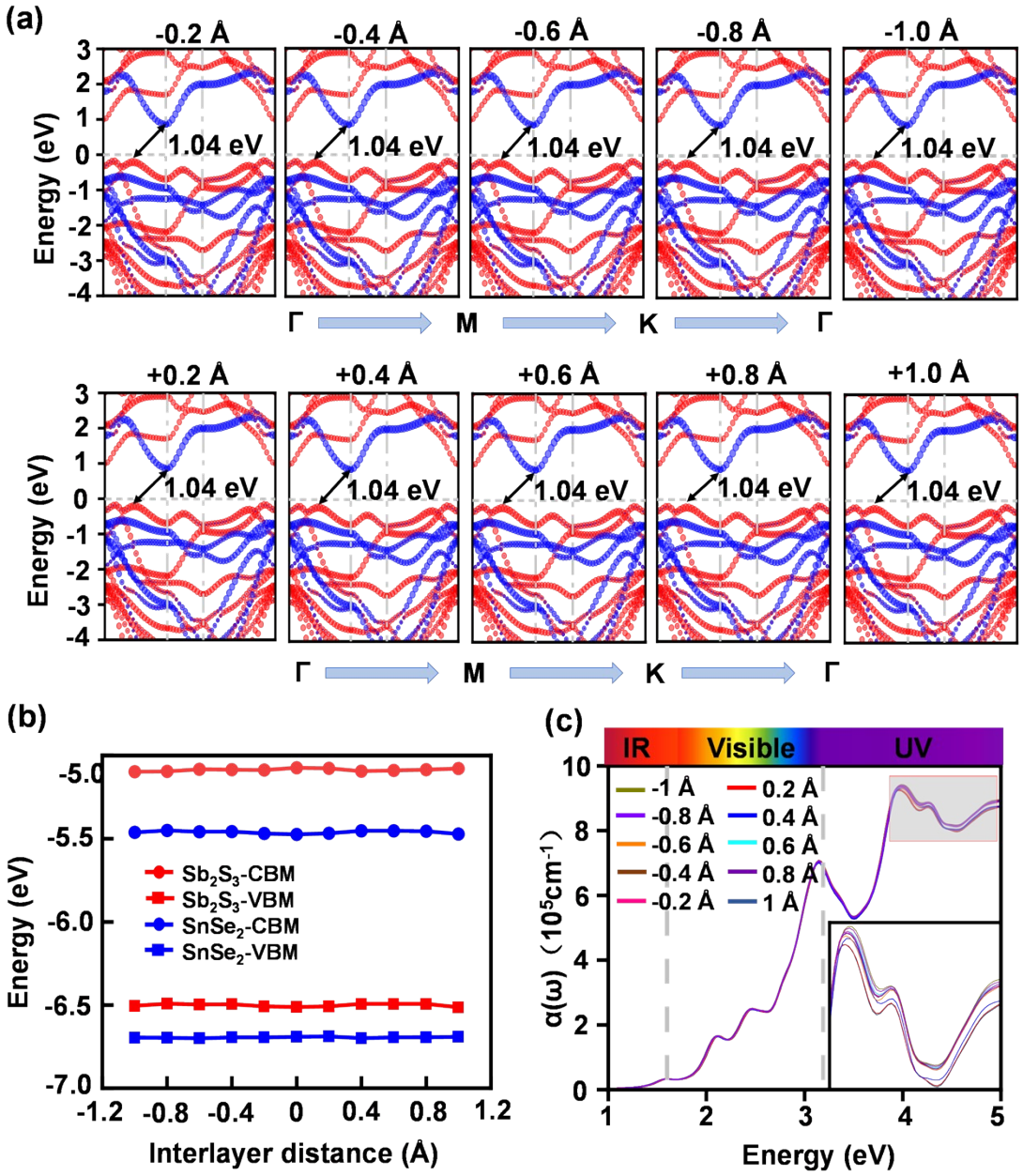

Figure S7. (a) Band structures of the $Sb_2S_3/SnSe_2$ heterostructure at different interlayer distances. Blue and red dots represent the projected states of $SnSe_2$ and Sb_2S_3 layers, respectively. (b) Evolution of the CBM and VBM positions of the individual sublayers as the interlayer distance varies from -1 Å to 1 Å. (c) Optical absorption spectra of the heterostructure under different interlayer spacings.

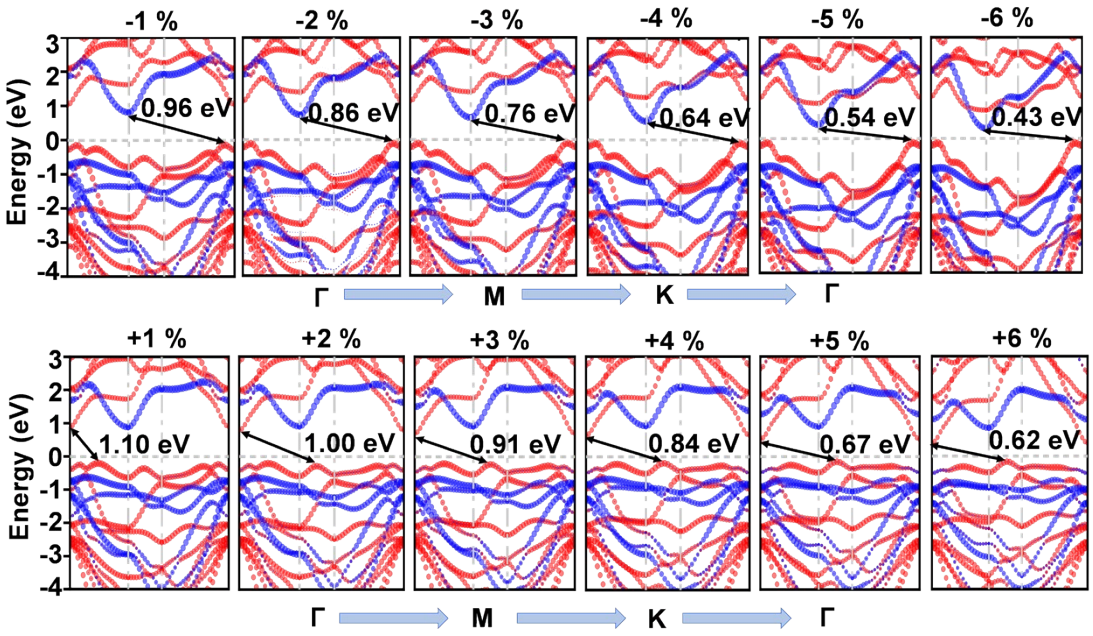

Figure S8 Band structures under different biaxial strains

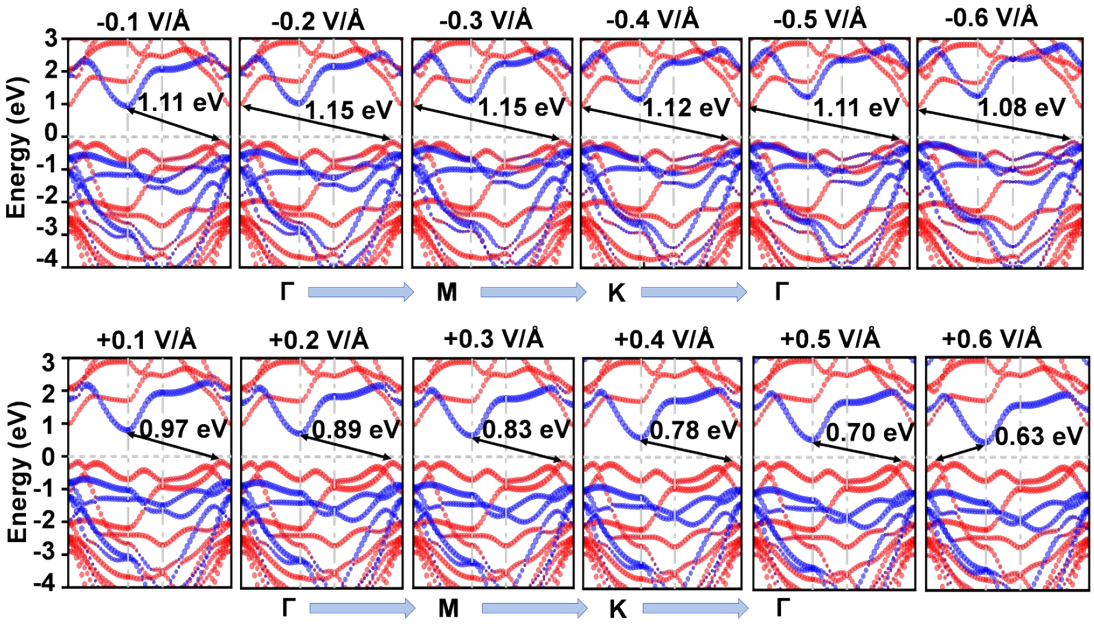

Figure S9 Band structures under different electric fields